

Simulation of galvanic corrosion of magnesium coupled to a steel fastener in NaCl solution

J. X. Jia, A. Atrens*, G. Song and T. H. Muster

The galvanic corrosion of magnesium alloy AZ91D coupled to a steel fastener was studied using a boundary element method (BEM) model and experimental measurements. The BEM model used the measured polarization curves as boundary conditions. The experimental program involved measuring the total corrosion rate as a function of distance from the interface of the magnesium in the form of a sheet containing a mild steel circular insert (5 to 30 mm in diameter). The measured total corrosion rate was inter-

preted as due to galvanic corrosion plus self corrosion. For a typical case, the self corrosion was estimated typically to be ~ 230 mm/y for an area surrounding the interface and to a distance of about 1 cm from the interface. Scanning Kelvin Probe Force Microscopy (SKPFM) revealed microgalvanic cells with potential differences of approximately 100 mV across the AZ91D surface. These microgalvanic cells may influence the relative contributions of galvanic and self corrosion to the total corrosion of AZ91D.

1 Introduction

The galvanic corrosion of magnesium alloys is a major concern in the application of magnesium in the automotive industry. Magnesium is the most active structural metal and thus would suffer serious galvanic corrosion when in contact with a different metal [1, 2]. More specifically, the galvanic corrosion of magnesium caused by fasteners is of the most concern in automotive applications. Many types of fasteners have been developed and several evaluations of the various fastener systems in terms of mass loss of magnesium have been reported by *Hawke and Ruden* [3], *Skar* [4] and *Gao et al.* [5]. *Skar* [4] showed that 6000 series aluminum alloy fasteners caused negligible galvanic corrosion of magnesium in salt spray test conditions. However, for many applications steel fasteners are desired due to their inherent mechanical properties. The use of steel fasteners with an aluminium plated coating has been shown to have poor compatibility with magnesium [5]. *Hawke and Ruden* [3] found steel fasteners with zinc or tin-zinc alloy coatings to have an effective compatibility with magnesium in salt water exposure.

In addition to characterizing galvanic corrosion by mass loss, the maximum depth of corrosion is also an important characteristic, which can be evaluated by an examination of the cross section corrosion penetration [5]. In neutral or alkaline salt solutions, the corrosion of magnesium alloys is characterized by pitting [6]. Stable corrosion pits have been observed to initiate at flaws adjacent to a fraction of

the intermetallic particles as a result of the breakdown of passivity. The pitting corrosion could occur in combination with the galvanic corrosion, and can be initiated by the galvanic corrosion.

The total corrosion in the area of galvanic corrosion can be considered to be made up of the following two components: (1) galvanic corrosion and (2) self corrosion [3-5]. In this approach the galvanic corrosion is defined as that part of the corrosion which is directly caused by the coupling of the magnesium to a steel fastener. The self corrosion is defined as the extra corrosion. Both the galvanic corrosion and the self corrosion may take the form of more or less general corrosion, or the form of localized corrosion or pitting corrosion. The total corrosion is often measured by mass loss of the test sample. The galvanic corrosion of specimens can be measured using various electrochemical methods as in our prior work [7-9], and can be modelled using numerical methods such as Boundary Element Methods as used in our prior work [7-11].

Astley [12, 13], *Fu* [14], *Adey* [15] and *Kasper* [16] have indicated that numerical methods are promising for the prediction of galvanic corrosion and more specifically, galvanic current distributions. With the development of computer technology, a boundary element based program, BEASY, has become widely used in galvanic corrosion studies since the early 1980s [17]. Our previous study showed the BEASY program to provide promising correlations with experimental data [7, 10]. In the present study the BEASY program was used to calculate the galvanic current distribution on magnesium alloy AZ91D surfaces. Based on our prior work [7-11], the expectation was that the BEASY program could provide a good prediction of the galvanic current distribution. In addition, the total corrosion was measured experimentally as a function of distance from the magnesium-steel interface.

AZ91D has a two-phase microstructure, consisting of a matrix of α grains and β -phase $Mg_{17}Al_{12}$ intermetallics [1, 2]. As a result, the localized potential differences resulting from the heterogeneous composition of the surface will influence both galvanic and self corrosion processes. In an effort to further understand the total corrosion and the galvanic corrosion caused by a steel fastener in 5% NaCl solution, information on the magnitude of localized potential differences was ob-

* A. Atrens, J. X. Jia, G. Song,
CRC for Cast Metals Manufacturing (CAST),
Division of Materials, School of Engineering,
The University of Queensland,
St Lucia, QLD 4072 (Australia)

T. H. Muster,
Corrosion Science and Surface Design,
CSIRO Manufacturing and Infrastructure Technology,
Graham Road, Highett, Victoria, 3190 (Australia)

tained by performing Scanning Kelvin Probe Force Microscopy (SPKFM) over the surface of AZ91D specimens.

2 Experimental approach

2.1 Galvanic corrosion assembly

HPDC AZ91D and mild steel were the test materials. Each galvanic assembly consisted of an 11 cm × 12 cm plate of AZ91D containing a mild steel circular insert in the center of the plate. The diameters of the mild steel inserts were 5 mm, 10 mm and 30 mm. The steel was insulated from the AZ91D by a thin layer of Teflon and molded in resin. The AZ91D plate and steel electrode were electrically connected by a wire and formed a galvanic couple.

2.2 Electrolytes

5% NaCl solution was used because it represents a severe corrosive environment. Also, previous studies have shown reasonable agreement between the BEM calculation and the experimental measurement using this electrolyte [7, 10]. That is, the galvanic current is stable and there is little corrosion product interference, which makes it easier to distinguish the effect of geometry. The 5% NaCl solution was made with analytical grade reagents and deionized water. The conductivity of the 5% NaCl solution, as measured using a platinum conductivity cell, was determined to be 79500 S · cm.

2.3 Corrosion assessment

After 48 hours of immersion test in a solution of 5% NaCl to a depth of 10 mm, the corrosion product was removed from the surface of each specimen. The corrosion morphology was recorded. Each specimen was sectioned into 8 pie-shaped pieces. The corroded area on each cross section was measured in 1 mm sections using an optical microscope and Leica Qwin image analysis software. The average corrosion rate for each sample was calculated by integrating the damage depth along the length of each cross section.

2.4 Polarization curve measurement

Fig. 1(a) presented the experimental arrangement for polarization curves measurement. Further detail on this technique can be found in previous studies [7, 10]. Both potentiodynamic and galvanostatic polarization curves were measured. The potentiodynamic curves provide an estimate of the current density values for the subsequent measurement of the galvanostatic polarization curves. For each applied constant current, the potential was measured as a function of time. The galvanostatic polarization curves were obtained by plotting the potential versus current density at 5 to 10 minutes for the 5% NaCl solution, when steady state had been attained. A 1287 electrochemical interface was used to measure the polarization curves. A REF201 Ag/AgCl reference electrode was used. To eliminate the influence of solution resistance on the measured polarization curve, the solution resistance was measured using a 1255B Frequency Response Analyzer. The polarization curves were corrected for potential drop caused by the solution resistance. The solution resistance corrected galvanostatic polarization curves for AZ91D and steel 4150 in 5% NaCl solution, were obtained by plotting current density versus potential. Fig. 1(b) provides a typical polarization curve.

2.5 AFM and SKPFM measurements

Atomic Force Microscopy (AFM) and Scanning Kelvin Probe Force Microscopy (SKPFM) investigations were performed on a Digital Instruments Nanoscope III Multimode instrument with an ExtenderTM electronics module. Contact potential differences were captured using a Lift-ModeTM height of 100 nm. To achieve acceptable tracking of the surface topography when using lift mode, a considerable contact force of up to 80 nN was applied between tip and sample, and scan rates as low as 0.4 Hz were used. Further operational details have been published elsewhere [18–21]. All contact potential differences presented in this study were scaled relative to the potential of a Pt-coated silicon cantilever tip (NT-MDT), and for ease of presentation, contact potential differences were plane-fitted and plotted with the most negative potential being the most noble.

For SKPFM analysis, six AZ91 samples with dimensions of 10 mm × 10 mm × 1 mm were cut from larger AZ91 blocks. The thin slices were polished using a sequence of diamond pastes (15 μm, 3 μm and 1 μm) and OP-S (Struers) oxide polish. After the final polish the samples were rinsed with deionised water, analytical grade ethanol and dried using high purity argon. Individual samples were then immersed in 5% NaCl solution for one minute, rinsed with deionised water and dried using high purity argon.

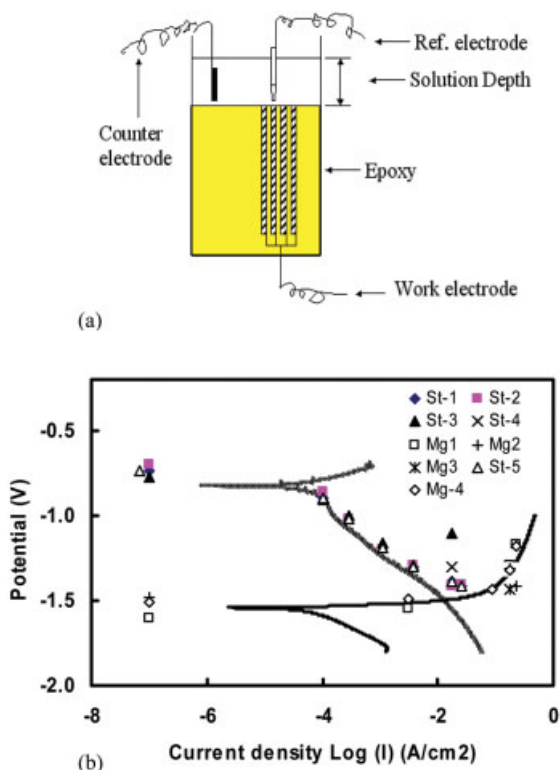


Fig. 1. (a). Schematic arrangement for measuring polarization curves; (b) Galvanostatic polarization curve measurements (data points) in 5% NaCl solution. Curves represent typical potentiodynamic polarization curves, at a scan rate of 2 mV/s

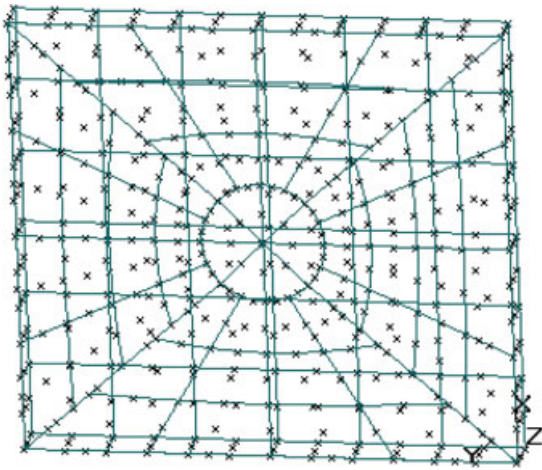


Fig. 2. Schematic of the mesh for the BEM model

3 BEM model

Three-dimensional BEM models were generated in the BEASY environment to represent the real specimens immersed in 10 mm 5% NaCl solution. The mesh sizes were defined by the minimum 0.1 cm to maximum 0.7 cm for all the three models. These dimensions were found to be fine enough to give reliable and reproducible galvanic current gradients. The tolerance of the potential was set as 0.01 mV. Fig. 2 illustrates the mesh for the galvanic specimen with $\phi = 30$ mm steel insert.

4 Results and discussion

4.1 Overview

Figs. 3a, 4a and 5a illustrate the physical appearance of the AZ91D plate after 48 hours immersion in 5% NaCl solution. The samples exhibited an unevenly distributed corrosion due to the galvanic couple with steel. Corrosion damage was deeper at the AZ91D-steel interface, and included pitting further away from the interface. Corrosion damage to AZ91D was concentrated around the steel and was largely confined to within about 1 to 2 cm radial distance from the interface. The radial extent of the corrosion was similar in all these cases. There were some pits distributed randomly out on the remaining surface of the AZ91D. However, most of the remaining area was free from corrosion and retained its original appearance. This indicated that the effective distance of galvanic corrosion was limited to a distance of 1 to 2 cm. Most of the remaining area seemed to be protected as a cathode. A similar finding was also reported by Hawke [22], who derived an effective insulating space of about 5 mm for magnesium coupled with cast iron.

Figs. 3 to 5 compare the overview of the physical appearance of the corrosion with the area of galvanic corrosion as simulated by the BEM model. This comparison shows that the computer model provided reasonable predictions of the effective galvanic corrosion area for each of the three different sizes of steel cathodes in 5% NaCl solution.

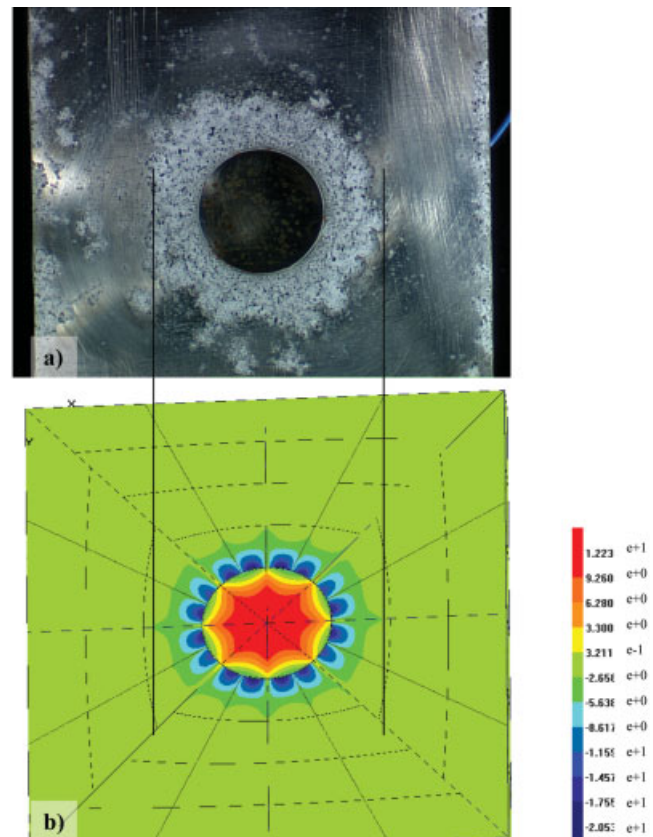


Fig. 3. Comparison of the galvanic corrosion area for the BEM model and the immersion test for 30 mm diameter steel cathode. a) experimental immersion test and b) the BEM model. The extent of the galvanic corrosion for the BEM model was estimated by the point where the galvanic current becomes essentially zero

4.2 Distribution of corrosion

Figs. 6 to 14 illustrate the typical distribution of total corrosion and provide a comparison between the total corrosion rate on the corroded area for each small cross section, and the galvanic current derived from the BEM modeling calculation for AZ91D coupled with 5 mm, 10 mm and 30 mm diameter steel inserts. The total corrosion rate for each small cross section was calculated from the corresponding measured corroded area. This total corrosion rate includes galvanic and self corrosion, both of which may be in the form of pitting corrosion and general corrosion.

Analysis of the cross sectional damage indicated that the corrosion of AZ91D included unevenly distributed pitting corrosion. The maximum corrosion depth occurred close to but not always immediately adjacent to the magnesium-steel interface as shown in Figs. 6, 7, 9, 10, 12 and 13. A similar finding was also reported by Ault [18]. The maximum depth occurred within about 1 mm away from the interface. The depth distribution of the galvanic pitting corrosion was quite randomly scattered on the surface and there was no obvious relationship between the depth and the pit location within a 2 cm distance.

Figs. 8 and 11 provide a comparison of the BEM model predicted galvanic corrosion and the experimental measurement of the total corrosion for AZ91D coupled with 5 mm and 10 mm steel inserts, respectively. Both the BEM model and the experimental measurements indicate maximum corrosion

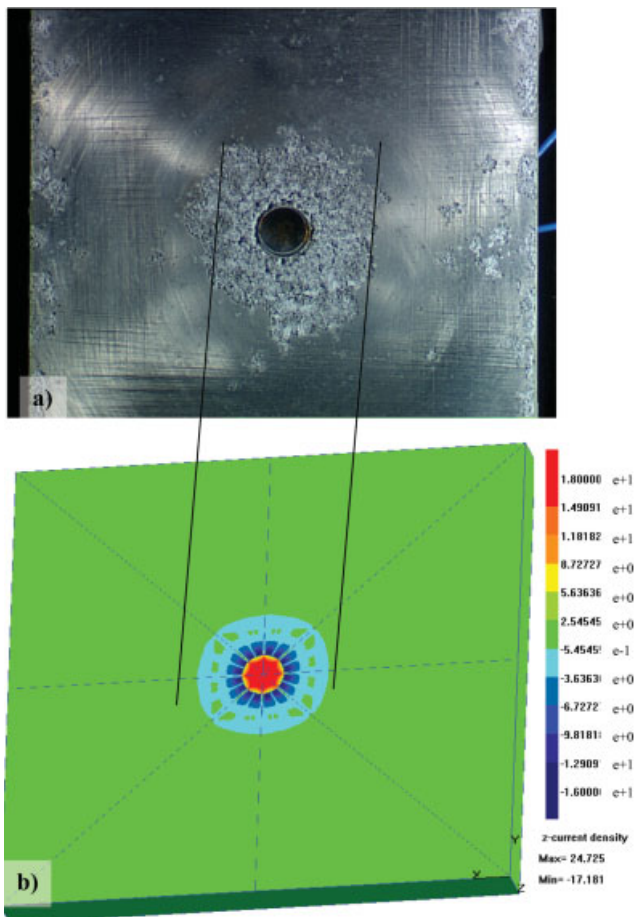


Fig. 4. Comparison of the galvanic corrosion area for BEM model and the immersion test for 10 mm diameter steel cathode. a) experimental immersion test and b) the BEM model. The extent of the galvanic corrosion for the BEM model was estimated by the point where the galvanic current becomes essentially zero

at the magnesium-steel interface, and both indicated a decrease in corrosion rate with increasing distance from the interface. The experimental measurements indicate a corrosion rate significantly higher than the galvanic corrosion rate, and this is interpreted as self corrosion of magnesium. This self corrosion was estimated by subtracting the galvanic corrosion (as predicted by the BEM model) from the total measured corrosion in Figs. 8 and 11. The value as estimated was 10 mA/cm² at the magnesium-steel interface and similar values were estimated at a distance of 1 cm from the interface. This self corrosion corresponds to a penetration rate of ~230 mm/y. Fig. 14 provides similar comparison for magnesium coupled to a 30 mm steel insert. In this case, there was reasonable agreement.

4.3 SKPFM investigation

Figs. 15 and 16 present the potential distribution on the surface of the magnesium alloy derived from SKPFM measurements. The average contact potential difference between the Pt tip and polished AZ91D was 1590 mV. This value decreased slightly to 1560 mV following a one minute exposure to 5% NaCl. Comparison of the potential maps and the microstructure led to the following interpretation. In the potential

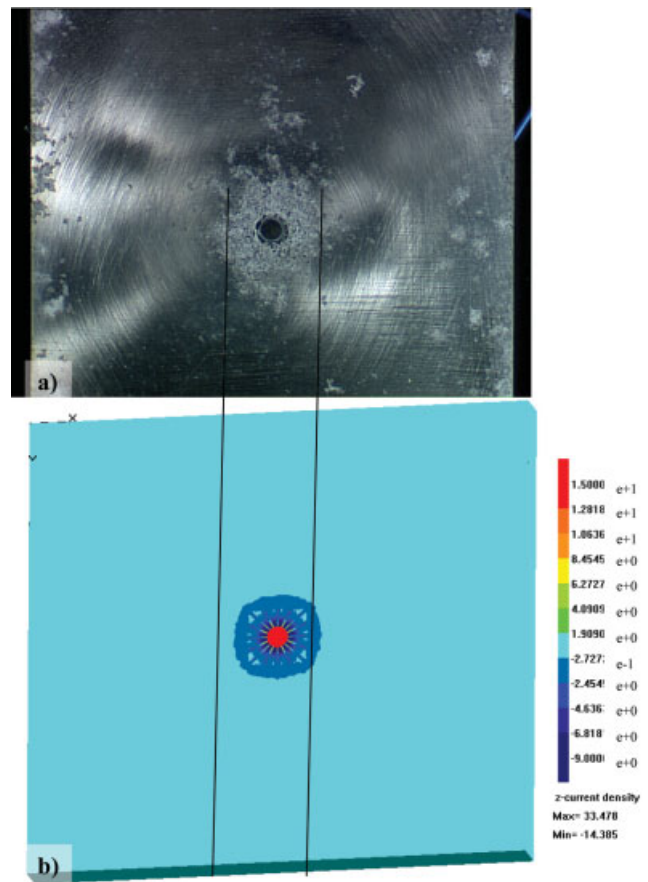


Fig. 5. Comparison of the galvanic corrosion area for the BEM model and the immersion test for 5 mm diameter steel cathode. a) experimental immersion test and b) the BEM model. The extent of the galvanic corrosion for the BEM model was estimated by the point where the galvanic current becomes essentially zero

maps the darker regions (corresponding to the β phase) exhibited a decreased contact potential difference in comparison to the surrounding matrix (α phase). For polished samples the contact potential difference between the α and β phases was as much as 145 mV with contact potential difference values of 1705 mV and 1560 mV for α and β phases, respectively. After exposure to 5% NaCl for one minute the difference in potential difference between α and β phases decreased to approximately 90 mV, with typical contact potential difference values of 1640 mV and 1550 mV for the α and β phases, respectively. The relationship between contact potential difference and electrochemical potentials has been explored previously by *Schmutz* and *Frankel* [20, 21]. They showed that a linear relationship existed between SKPFM measured contact potential difference values (which were measured in air) and the corrosion potential measured in NaCl aqueous solution. Therefore, contact potential difference measurements provide a platform in which to investigate local galvanic interactions on metallic surfaces. The current study indicates that the β phase has increased nobility in comparison to the α phase. Similar conclusions have been reported by *Song*, *Atrrens*, and *Dargusch* [23]. This suggests that micro-galvanic cells may be formed between the β phase and α phase. The galvanic corrosion or pitting can be initiated and developed at the flaws next to the β phase particles and can cause accelerated corrosion of the α phase. The size, distribution and potential differences of the micro-galvanic cells associated with the β phase



Fig. 6. Image of corrosion on Mg surface coupled with 5 mm diameter steel insert (side 1)

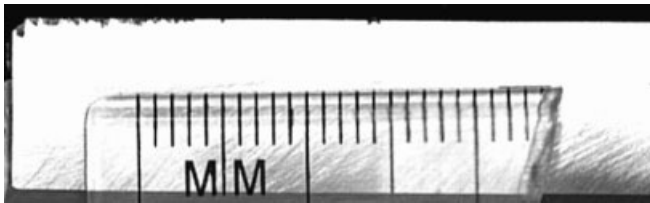


Fig. 7. Image of corrosion on Mg surface coupled with 5 mm diameter steel insert (side 2)

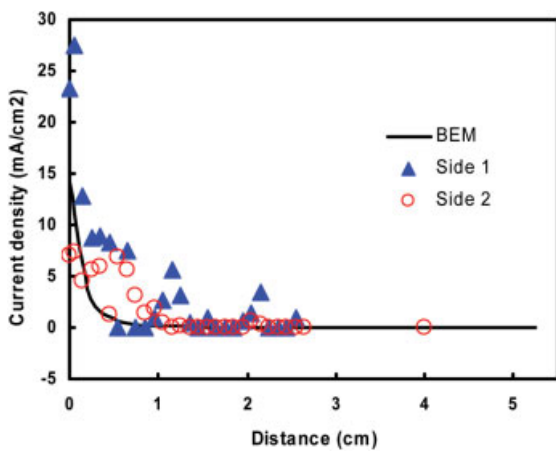


Fig. 8. Comparison of corrosion current density between the BEM model and the experiments for Mg coupled with 5 mm diameter steel insert

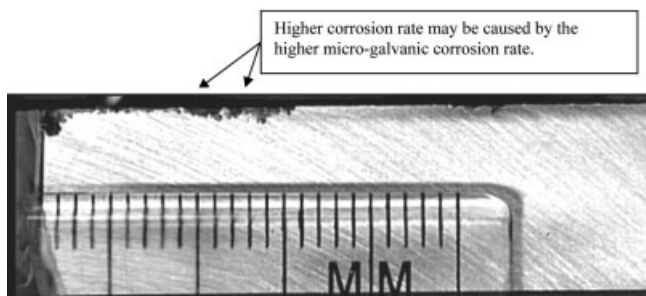


Fig. 9. Image of corrosion on Mg surface coupled with 10 mm diameter steel insert (side 1)

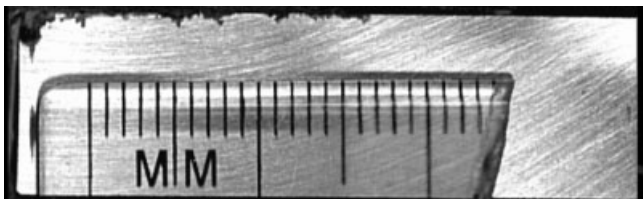


Fig. 10. Image of corrosion on Mg surface coupled with 10 mm diameter steel insert (side 2)

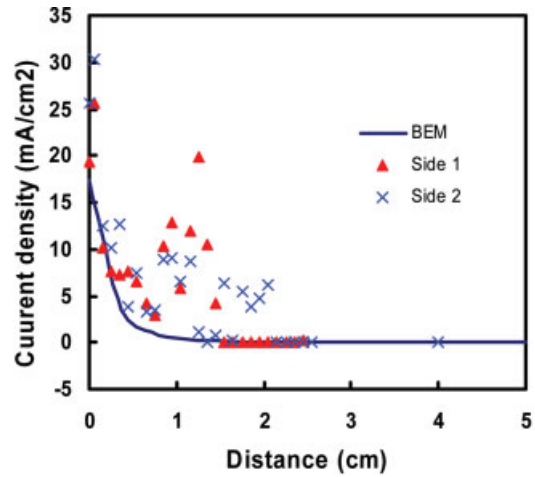


Fig. 11. Comparison of corrosion current density between the BEM model and the experiments for Mg coupled with 10 mm diameter steel insert

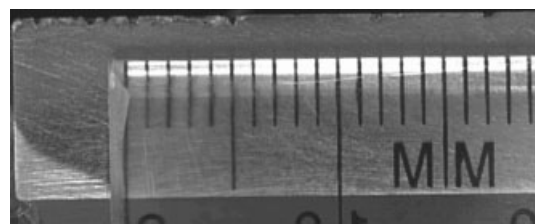


Fig. 12. Image of corrosion on Mg surface coupled with 30 mm diameter steel insert (side 2)

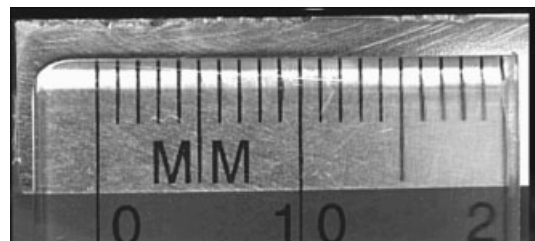


Fig. 13. Image of corrosion on Mg surface coupled with 30 mm diameter steel insert (side 1)

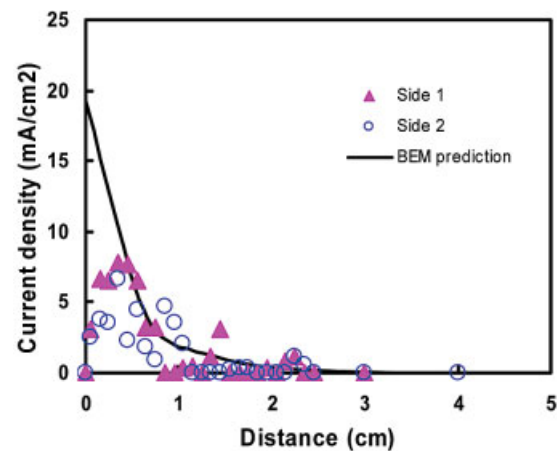


Fig. 14. Comparison of corrosion current density between the BEM model and the experiments for Mg coupled with 30 mm diameter steel insert

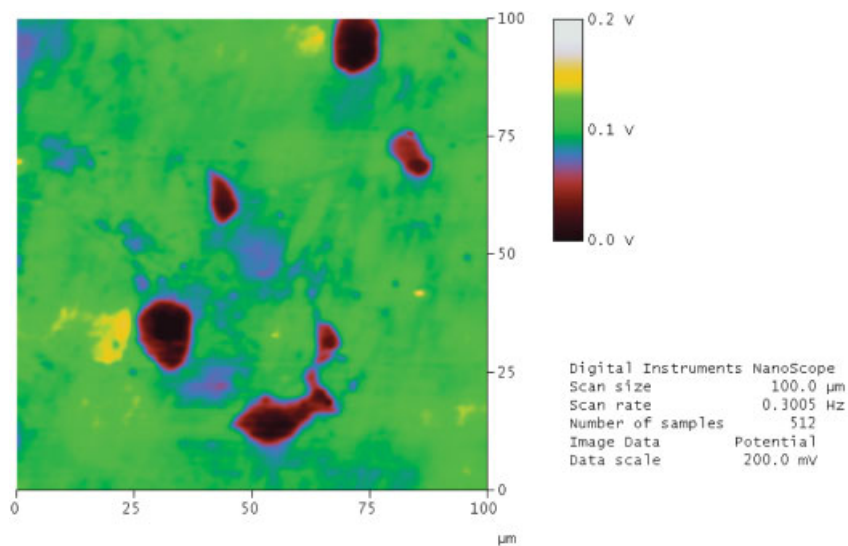


Fig. 15. A representative contact potential difference map for the SKPFM of magnesium alloy AZ91D after immersion in 5% NaCl for one minute

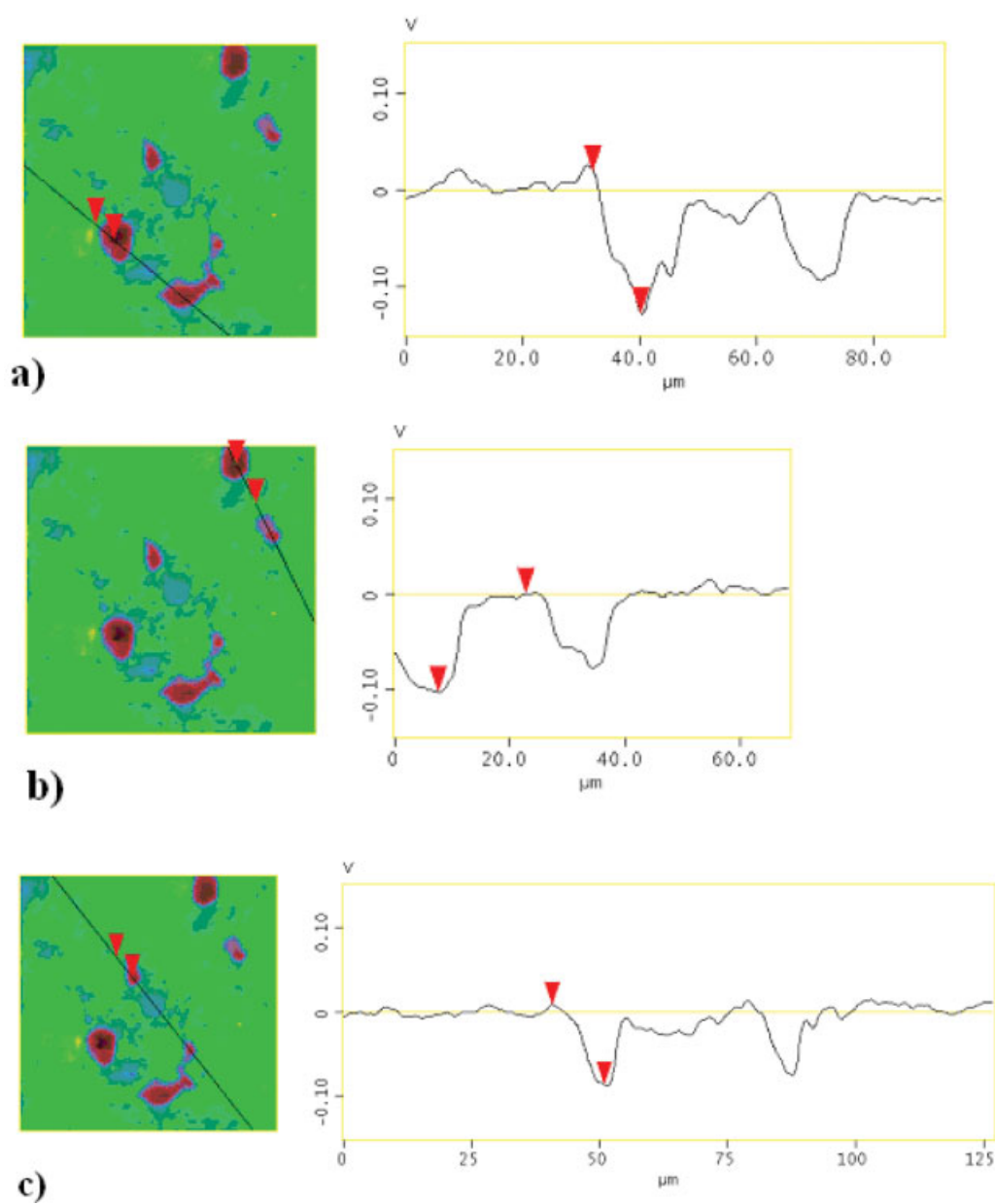


Fig. 16. (a), (b) and (c) show cross sections of the potential along sections representing the surface of AZ91D, as per Fig. 15

particles may influence self corrosion rates, may also influence galvanic corrosion rates and ultimately determine the relative contributions to the total corrosion rate. The corrosion rate could be higher if the micro-galvanic corrosion rate is high for some locations which can be far away from the steel as illustrated in Fig. 9. This effect is not taken into account in the BEM model.

5 Conclusion

Both the BEM model and the experimental measurements of the galvanic corrosion of AZ91D coupled to steel predicted a similar distribution of the current density: a maximum at the interface and decreasing rapidly to zero within 1 to 2 cm from the interface.

The total corrosion was interpreted as being due to galvanic corrosion plus self corrosion. The self corrosion was evaluated on the basis that the BEM model provides a good evaluation of the galvanic corrosion. On this basis, the self corrosion rate was evaluated to be typically ~ 230 mm/y for the area surrounding the interface and to a distance of about 1 cm from the interface. Self corrosion rates may be controlled by localized microgalvanic corrosion processes. SKPFM confirmed the presence of microgalvanic cells on the surface of AZ91D, which appear to have potential differences in the order of 100 mV between phases in the alloy.

6 References

- [1] G. Song, A. Atrens, *Advanced Engineering Materials* **2003**, *5*, 837.
- [2] G. L. Song, A. Atrens, *Advanced Engineering Materials* **1999**, *1*, 11.
- [3] D. Hawke, T. Ruden, *Society of Automotive Engineers*, [Special Publication] SP, **1995**, SP-1096, 63–67.
- [4] J. I. Skar, *Materials and Corrosion* **1999**, *50*, 2.
- [5] G. Gao et al. in: *The 2nd Israeli International Conference on Magnesium Science & Technology* **2000**, Dead Sea, Israel.
- [6] E. Ghali, *Magnesium Alloys*, **2000**, 350–3, 261.
- [7] J. X. Jia, G. Song, A. Atrens, *Materials and Corrosion* **2005**, *56*, 259.
- [8] J. X. Jia, G. Song, A. Atrens, G. Chandler, D. H. StJohn, in: *The First International Light Metals Technology Conference* **2003**, Brisbane, Australia, 397–400.
- [9] J. X. Jia, G. Song, A. Atrens, D. H. StJohn, J. Baynham, G. Chandler, *Materials and Corrosion* **2004**, *55*, 845.
- [10] J. X. Jia, G. Song, A. Atrens, *Corrosion Science*, submitted for publication.
- [11] J. X. Jia, G. Song, A. Atrens, D. H. StJohn, in: *13th Asian-Pacific Corrosion Control Conference*, **2003**, Osaka, Japan. Japan Society of Corrosion Engineering, 34.
- [12] D. J. Astley, *Chem. Ind. (London)* **1977**, *13*, Suppl., Seawater Cool. Chem. Plant, 4.
- [13] D. J. Astley, *ASTM Spec. Tech. Publ.* **1988**, 978 (Galvanic Corros.), 53–78.
- [14] J. W. Fu, *ASTM Spec. Tech. Publ.*, **1988**, 978 (Galvanic Corros.), 79–95.
- [15] R. A. Adey, S. M. Niku, *ASTM Spec. Tech. Publ.*, **1988**, 978 (Galvanic Corros.), 96–117.
- [16] R. G. Kasper, E. M. Valeriotte, *Galvanic Corrosion*, ed. H. P. Hack. **1988**, Philadelphia, American Society for Testing and Material.
- [17] H. P. Hack, *Corros. Rev.*, **1997**, *15*, 195.
- [18] P. Campestrini et al., *Surface and Coatings Technology* **2004**, *176*, 365.
- [19] V. Guillaumin, P. Schmutz, G. S. Frankel, *Journal of the Electrochemical Society* **2001**, *148*, B163.
- [20] P. Schmutz, G. S. Frankel, *Journal of the Electrochemical Society* **1998**, *145*, 2295.
- [21] P. Schmutz, G. S. Frankel, *Journal of the Electrochemical Society* **1998**, *145*, 2285.
- [22] D. L. Hawke, in: *14th International DieCasting Congress and Exposition* **1987**. Toronto, Ontario, Canada.
- [23] G. Song, A. Atrens, M. Dargusch, *Corros. Sci.* **1999**, *41*, 249.

(Received: December 13, 2004)

W 3855